

# Multi Tbit/in<sup>2</sup> storage densities with thermo-mechanical probes

D. Wiesmann,<sup>†</sup> C. Rawlings,<sup>†</sup> R. Vecchione,<sup>‡</sup> F. Porro,<sup>‡</sup> B. Gotsmann,<sup>†</sup> A. Knoll,<sup>†</sup>  
D. Pires,<sup>†</sup> and U. Duerig<sup>\*,†</sup>

*IBM Research GmbH, Saemmerstrasse 4, 8803 Rueschlikon, Switzerland, and  
STMicroelectronics, P.le Enrico Fermi 1, Porto del Granatello, 80055 Portici (NA), Italy*

E-mail: drg@zurich.ibm.com

## Supporting Information Available

### Polymer

The polymer used is a Polyaryletherketone (PAEK), shown in Figure 1, incorporating diresorcinnol units in the backbone for control of the glass-transition temperature (T<sub>g</sub>) and phenyl-ethynyl groups in the backbone and as endgroups for cross-linking functionality. These polymers exhibit excellent thermal stability up to 450°C. The polymer used here was specifically tailored for probe-storage applications, and has 18% of phenyl-ethynyl groups in the backbone to enhance the overall cross-linking. The molecular weight is approximately 5.5 kDa, and a T<sub>g</sub> of 150°C is measured by dynamic scanning calorimetry. Unlike homopolymer films, such chemically cross-linked polymers are stable against repetitive imaging in contact-mode scanning probe microscopy.<sup>1,2</sup> Thin films are

---

<sup>†</sup>IBM-Research

<sup>‡</sup>STMicroelectronics

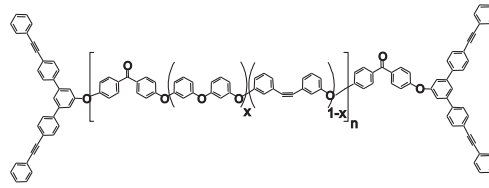


Figure 1: Molecular structure of the Polyaryletherketone (PAEK) polymer

prepared by spin-casting from anisole solution. To induce the cross-linking reaction, the films are cured at 400°C for 1 h in nitrogen atmosphere. Homogeneous films are obtained, with average thicknesses of 120 nm, as measured by ellipsometry, by using solutions of 5% wt.

## Templating

A freshly cleaved mica sheet (muscovite mica Grade V1 obtained from SPI Supplies) is used as template. The square mica samples,  $2.5 \times 2.5 \text{ cm}^2$  in size, are mechanically cleaved. Typically fewer than three large steps are observed by optical inspection throughout the sample area, resulting in atomically flat surfaces in between the steps, which are in the square centimeter range. First, a thin film of polymer is spin-cast and cured on a freshly cleaved mica substrate, which serves as the template. Then, a silicon wafer, referred to as "target", is put into contact with the free surface of the polymer. The sandwich is clamped using tweezers and applying moderate pressure, and submerged in ultra-pure water. As mica is highly hydrophilic, water penetrates between the mica and the polymer surfaces, thereby releasing the polymer film. The transfer to the target substrate is assisted if hydrophobic hydrogen-terminated silicon wafers or polymer-coated wafers are used as targets. In this case, the water does not penetrate between the polymer and target surface, and the transfer completes over the full area in less than one minute. After lifting off the mica substrate, the templated polymer surface is exposed.

## Thermomechanical Writing and Reading

The indentation experiments reported here were performed using home-built equipment. A cantilever-style probe sensor made of silicon (Si), which comprises a capacitive platform for exerting a loading force by electrostatic means and a resistive heater for heating of the tip integrated on top of the heater.<sup>3,4</sup> The cantilevers used in the experiments have a spring constant of 0.1+0.1/-0.05 N/m and a lowest resonance frequency of 60 kHz. The indenter tip is of conical shape with a cone aperture varying between 38° and 55° and an apex radius of less than 10 nm. The tip is heated by applying an appropriate voltage to the resistive heater element, and the temperature is determined from the measured electrical resistance and using the known temperature dependence of the resistivity of doped Si.<sup>4,5</sup> The electrostatic load force is calibrated in an independent experiment by measuring the lever deflection as a function of the applied potential.

Scanning of the tip is accomplished using a linearized commercial piezo scanner (Physical Instruments P-733-2D). The typical scan speed and scan range are 0.1 mm/s and 5  $\mu$ m, respectively. A constant offset is added at the beginning of a line scan, which provides a discrete sampled scan in the second dimension. The tip rests in a stand-by position 300 nm above the polymer surface. To form an indent, electrostatic force pulses, in the range from 100 to 500 nN and heater voltage pulses that raise the heater temperature up to 500°C, are simultaneously applied for a duration of 5  $\mu$ s. The electrostatic force brings the tip into contact with the polymer surface and provides the indenter load force. The hot tip locally heats the polymer, thereby facilitating indentation. The temperature of the polymer under the tip can only be inferred indirectly from the heater temperature. Empirically it is found that the effective temperature increase with respect to the room temperature in the polymer amounts to approximately 0.3 - 0.6 times the temperature increase measured in the heater (for details see Refs<sup>4,6</sup>). The indentation terminates when the heating of the indenter tip and the capacitive loading force are switched off, which causes the cantilever to snap back to its rest position above the surface. The mechanical response time of the cantilever is below 1  $\mu$ s,<sup>7</sup> and the thermal response time for heating is of the same order of magnitude.<sup>5</sup>

Imaging of the polymer surface is performed using the same cantilever tip as used for writing

the indents. The instrument is operated in contact imaging mode using contact forces on the order of 10 nN and a scan speed of 0.1 mm/s. No feedback is used to control the height of the cantilever base over the surface. The soft cantilever spring compensates for the topographic modulation of the sample surface, and the vertical displacement of the tip is directly measured via an integrated thermal sensor which is thermally decoupled from the tip.<sup>3</sup> The peak-to-peak height modulation of the samples investigated here is below 10 nm, and the tilt of the surface plane can be corrected to contribute less than 10 nm of modulation to the out-of-plane component. Therefore, the load force on the tip varies by less than 5 nN. The response time of the thermal read sensor is on the order of 20  $\mu$ s<sup>6</sup> which is substantially faster than the typical sampling rate of 10 kHz during topographic imaging.

### Correlation between rim radius $c$ and indent radius $a$

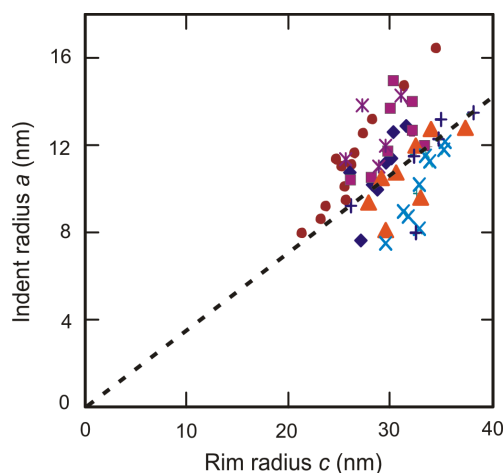


Figure 2: Indent radius,  $a$ , versus rim radius,  $c$ , measured for indents written into PAEK polymer samples. The different symbols correspond to different indenter tips and heater temperatures used for writing. Dashed line: Linear fit with  $c = 3a$ .

We have shown that the concept of self-similarity can be applied to nano-indents written into highly cross-linked polystyrene films.<sup>8</sup> Self-similarity predicts that vertical dimensions, e.g. the rim height, scale proportionally to the indent depth and lateral dimensions, e.g. the rim radius, scale proportionally to the indent radius. The scaling prediction also holds for indents written into

the PAEK polymer. Figure 2 shows the correlation between the indent radius,  $a$ , and the rim radius,  $c$ . The dashed line represents a linear scaling law,  $c = k_p a$ , with  $k_p = 3$ . The different symbols correspond to indents written using different indenter tips and heater temperatures as explained in the paper.

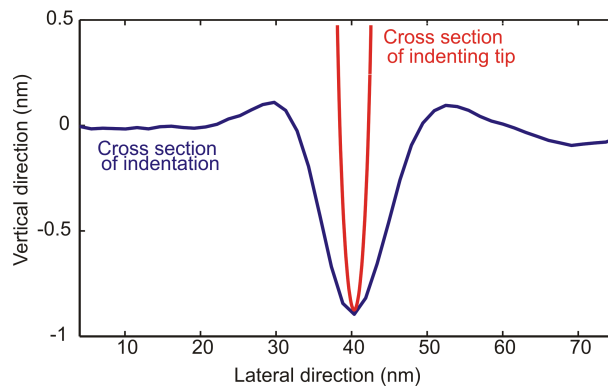


Figure 3: Cross section of the indenting tip based on TEM measurements (red) and an indent written and read with this tip (blue). The width of the indent significantly exceeds the width of the indenter as a result of a vertical recovery of the elastic deformation upon removal of the indenter. Therefore, the convolution effects from reading the indent with the indenting tip are negligible for the determination of indentation depth  $d$  and outer radius  $c$  within the measurement accuracy of about 5 - 10%.

One last point that needs to be scrutinized is the tip convolution effect, in particular when the same tip is used for creating and analyzing the indent. In this case several scenarios are possible, the indent is narrower than the tip because of predominantly horizontal indent relaxation after tip removal, the indent has a similar shape as the tip, or the indent is wider than the tip because of predominantly vertical relaxation upon tip removal. In the former two cases the analyzing the indent with the indenting tip would lead to an incorrect measurement of the inner radius and depth of the indent. On the other hand, if the indent predominantly relaxes in the vertical direction and if thus the indent is wider than the tip, the impact of the tip shape is reduced and is the lower the higher the relaxation. As described in Refs<sup>8,9</sup> the relaxation of thermo-mechanically written indents, both the elastic and plastic (over time) deformation, happens in the vertical ( $z$ ) direction only: the inner indent radius stays constant over the course of the bit relaxation while the depth decreases. This vertical deformation relaxation leads to an indent shape of significantly

larger width than the tip as illustrated in Figure 3 which shows a 0.9 nm deep indent (blue line) created with the sharpest tip, referred to as tip 1 in the paper together with the shape of the tip as determined by TEM (red line). As is obvious from the figure, the impact of the finite tip shape can be neglected for the determination of the outer indent radius  $c$  and the indent depth  $d$  in view of the overall measurement noise of 5 - 10%. The only critical quantity is the indent radius, which is systematically underestimated by approximately 30% of the indenter radius, and one tends to overestimate the numerical value of the corresponding scale constant  $k_p$ .

## References

- (1) Gotsmann, B.; Duerig, U.; Sills, S.; Frommer, J.; Hawker, C. *Nano Lett.* **2006**, *6*(2), 296–300.
- (2) Altebaeumer, T.; Gotsmann, B.; Pozidis, H.; Knoll, A.; Duerig, U. *Nano Lett.* **2008**, *8*(12), 4398–4403.
- (3) Pozidis, H.; Häberle, W.; Wiesmann, D. W.; Drechsler, U.; Despont, M.; Albrecht, T.; Eleftheriou, E. *IEEE Transactions on Magnetics* **2004**, *40*(4), 2531–2536.
- (4) Gotsmann, B.; Duerig, U. *Nano-Thermomechanics: Fundamentals and Application in Data Storage Devices*; Springer Heidelberg, 2006; Applied Scanning Probe Methods, ed B. Bhushan and H. Fuchs; Vol. IV.
- (5) Dürig, U. *Journal of Applied Physics* **2005**, *98*, 044906.
- (6) Gotsmann, B.; Lantz, M.; Knoll, A.; Duerig, U. *Nanoscale Thermal and Mechanical Interactions Studied using heatble Probes*; Wiley-VCH Weinheim, 2008; Nanotechnology, ed B. H. Fuchs; Vol. 6: Nanoprobes.
- (7) Gotsmann, B.; Rothuizen, H.; Duerig, U. *Appl. Phys. Lett.* **2008**, *93*, 093116.
- (8) Altebaeumer, T.; Gotsmann, B.; Knoll, A.; Cherubini, G.; Duerig, U. *Nanotechnology* **2008**, *19*, 475301.

- (9) Knoll, A.; Wiesmann, D.; Gotsmann, B.; Duerig, U. *Phys. Rev. Lett.* **2009**, *102*, 117801.